

## Recent advances in organic spin-valve devices

Fujian Wang, Z. Valy Vardeny\*

*Department of Physics, University of Utah, Salt Lake City, Utah 84112, USA*

Organic Spintronics has been considered to be the physics and applications of spin polarized electron injection, transport, manipulation and detection in organic diodes by the application of an external magnetic field. The prototype device is the organic spin-valve (OSV), which is based on an organic semiconductor spacer placed in between two ferromagnetic electrodes having different coercive fields, of which magnetoresistance changes with the applied field. Immense progress has been achieved in the past few years in fabricating, studying and understanding the underlying physics of these devices. We highlight the most significant advance in OSV research at the University of Utah, including the magnetoresistance response temperature and bias voltage dependencies; and show significant room-temperature operation using LSMO/C<sub>60</sub>/Co structure. We also report positive OSV-related magnetoresistance at low temperature, which was achieved using LSMO/polymer/Co OSV structure, where the polymer is a poly[phenylene-vinylene] derivative.

**Key Words:** Organic Spintronics, organic spin-valve, spin polarized carrier injection, magnetoresistance

\* To whom correspondence should be addressed; e-mail: [val@physics.utah.edu](mailto:val@physics.utah.edu)

## 1. Introduction

Extensive research in exploring the electron spin degree of freedom for the design of new electronic devices has occurred during the past dozen years. This interest has been motivated from the prospect of using spin and charge degrees of freedom, as information carrying physical quantity in electronic devices; thus expanding the device functionality in a new direction, which was dubbed *Spintronics* [1, 2]. This interest has culminated by awarding the 2007 Nobel Prize in Physics to Drs. Fert and Grünberg for the discovery and application of the Giant Magnetoresistance (GMR). More recently the Spintronics field has focused on hybrids of ferromagnet electrodes and semiconductors; however spin injection into a semiconductor has been a challenge [3]. In general, there are two methods by which spin aligned carriers can be generated in a semiconductor film. These are: optically, via the absorption of circularly polarized light in a direct-gap semiconductor such as GaAs; and spin injection from a ferromagnet (FM) electrode into a semiconductor overlayer. Here we focus on the latter method.

Key requirements for success in engineering spintronics devices using spin injection via FM electrode in a diode (or junction) are as following [2, 3]: efficient injection of spin polarized (SP) charge carriers through one device terminal (i.e. FM electrode) into the semiconductor interlayer; efficient transport and sufficiently long spin relaxation time within the semiconductor spacer; effective control and manipulation of the SP carriers in the structure; and effective detection of the SP carriers at a second device terminal (by another FM electrode). Traditional FM metals have been used as SP carrier injectors into semiconductors; however more recently magnetic semiconductors have been suggested for spin-injector, because of the existence of a conductivity mismatch between metallic FM and semiconductor interlayer. The conductivity mismatch was thought to be less severe using organic semiconductors (OSEC) as the medium in which spin-aligned carriers are injected, since carriers are injected into the OSEC by tunneling, and the tunnel barrier may be magnetic field dependent [3]. Spin relaxation lifetimes in conventional,

inorganic semiconductors are primarily limited by the spin-orbit interaction [1, 2]. However, OSEC are composed of light elements such as carbon and hydrogen that have weak spin-orbit interaction; and consequently are thought to possess long spin relaxation times [4, 5]. Therefore OSEC offer significant potential applications for spintronic devices [5, 6].

Figure 1(a) inset schematically shows a very useful spintronic device, namely the *spin valve* [7, 8]. Two FM electrodes (in this example  $\text{La}_{2/3}\text{Sr}_{1/3}\text{MnO}_3$  (LSMO) and Co, respectively [8]), serve as spin injector and spin detector, respectively are separated by a non-magnetic spacer (which in OSV devices is an OSEC layer). By engineering the two FM electrodes so they have different coercive fields ( $H_c$ ), their relative magnetization directions may switch from parallel (P) to anti-parallel (AP) alignment (and vice versa) upon sweeping the external magnetic field,  $H$  (see Fig. 1(b)). The FM electrode capability for injecting SP carriers depends on its interfacial spin-polarization value,  $P$ , which is defined in terms of the density,  $n$  of carriers close to the FM metal Fermi level with spin up,  $n^\uparrow$  and spin down,  $n^\downarrow$ ; given by the relation:  $P = [n^\uparrow - n^\downarrow] / [n^\uparrow + n^\downarrow]$ . The spacer decouples the FM electrodes, while allowing spin transport from one contact to the other. In this configuration the device electrical resistance depends on the relative orientation of the two FM electrode magnetizations. The electrical resistance is usually higher for the AP magnetization orientation, an effect referred to as GMR [1], which is due to spin injection and transport through the spacer interlayer. The spacer usually consists of a non-magnetic metal, semiconductor, or a thin insulating layer (in the case of a magnetic tunnel junction). The magnetoresistance (MR) effect in the latter case is referred to as tunnel magnetoresistance (TMR), and does not necessarily show spin injection into the spacer interlayer as in the case of the GMR response discussed before. Semiconductor spintronics is very promising field, because it allows for electrical control of the spin dynamics; and due to the relatively long spin relaxation time, multiple operations on the spins can be performed when they are out of equilibrium participating in transport of SP carriers [9]. Such a device based on FM/semiconductor/FM



geometry (for instance GaAs as a spacer [10]) may have other interesting optical properties, such as circular polarized emission that can be controlled by an external magnetic field [11].

Significant spin injection from FM metals into nonmagnetic semiconductors is challenging, because carrier density with spin-up and spin-down are equal in thermal equilibrium, and thus no spin polarization exists in the semiconductor layer. For achieving SP currents the semiconductor needs be driven far out of equilibrium, into a situation characterized by different quasi-Fermi levels for spin-up and spin-down charge carriers. Early calculations of spin injection from a FM metal into a semiconductor showed [12-15] that the large difference in conductivity of the two materials inhibits the creation of such a situation that blocks efficient spin injection into semiconductors; this has been known in the literature as the “conductivity mismatch” problem. However, a tunnel barrier contact between the FM metal and the semiconductor may help achieving significant spin injection [16]. The tunnel barrier contact can be formed, for example by adding a thin insulating layer between the FM metal and the semiconductor [17]. Tunneling through a potential barrier from a FM contact is spin selective because the barrier transmission probability, which dominates the carrier injection process into the semiconductor spacer, depends on the wave functions of the tunneling electron in the contact regions [3]. The wave functions in FM materials are different for spin-up and spin-down electrons at the Fermi surface, which are referred to as ‘majority’ and ‘minority’ carriers, respectively, and this contributes to their spin injection capability through a tunneling barrier layer.

## 2. Organic spin-valves experiments

### (i) The canonical OSV measurements

Evidence for large MR in OSV devices has been reported during the last few years [8, 16-27]. In the experimentally explored structures, most FM electrodes were made of the half-metal LSMO

that has spin polarization,  $P \sim 95\%$  [29] (see Fig. 1(b)); such devices showed a substantial GMR response up to 40% at low temperatures [8], even that tunnel barriers were not used. However the GMR response was found to substantially decrease with temperature and biasing voltage [8, 23]. Other OSV devices were fabricated from more conventional FM electrodes such as Co and Fe, which have not shown as large MR response as the former OSV devices [16, 24, 27, 28]; or not at all [30]. In few reports it was demonstrated that the MR response in polymer OSV [19, 25] and small molecules [17, 20] survives up to room temperature. In addition, it was also shown that organic diodes based on one FM electrode (namely, LSMO) possess another MR response at high fields, which may be intimately related to the LSMO electrode magnetic properties [8, 31].

Figure 1(b) shows [23] a typical MR loop at low  $H$  obtained with LSMO/CVB/Co spin-valve device at  $T = 14\text{K}$  and bias voltage of  $V \sim 10\text{ mV}$  positively applied to the LSMO electrode; CVB, or 4,4'-bis-(ethyl-3-carbazovinylene)-1,1'-biphenyl is an emissive oligomer of which molecular structure is shown in Fig. 1(a) inset. The arrows in Fig. 1(b) show the relative in-plane magnetization directions of the LSMO and cobalt electrodes, respectively upon sweeping  $H$ . It is seen that  $R(\text{AP}) < R(\text{P})$ , where  $R(\text{AP})$  [ $R(\text{P})$ ] is the device electrical resistance in the anti-parallel [parallel] electrodes magnetization orientation. This is opposite to many other metallic spin-valves, and was explained as due to the different  $P$  signs of the two FM electrodes in these devices [8, 32]. In agreement with this hypothesis it is noteworthy that a positive MR response was reported for OSV based on Co/Alq<sub>3</sub>/Py tunnel junction [24] [where Alq<sub>3</sub> is 8-hydroxyquinoline aluminum], in which  $P$  of both FM electrodes have the same sign. The obtained spin-valve related MR value ( $\text{MR}_{\text{SV}}$ ) in the device shown in Fig. 1, defined as  $\text{MR}_{\text{SV}} = \max\{[R(\text{P}) - R(\text{AP})]/[R(\text{AP})]\}$  at low  $H$  ( $< 1\text{ kG}$ ) was inferred from the MR response to be about 11%. It was also verified that the OSV device switched resistance values at  $H_{c1} \sim 50\text{ Oe}$  and  $H_{c2} \sim 600\text{ Oe}$ , in agreement with the respective coercive fields of the LSMO and Co electrodes measured using the magnetic optical Kerr effect [8, 23].

### (ii) Magnetoresistance bias voltage dependence

The  $MR_{SV}$  value in many OSV was found to decrease at large bias,  $V$  [8, 23, 27], as seen in Fig. 2 for the OSV device shown in Fig. 1. It is seen that  $MR_{SV}$  monotonically decreases with  $V$ . However it decreases less at negative  $V$ , where electrons are injected from the LSMO electrode into the OSEC interlayer; this apparent asymmetry is reduced when the MR is plotted vs. the current density in the device [23]. The  $MR_{SV}$  dependence on  $V$  is seen to be the same at the two measured temperatures, in spite of the apparent current increase obtained at the higher  $T$  (Fig. 1(a)). Similar MR decrease with  $V$ , including the polarity asymmetry has been measured in numerous LSMO/Co-based OSV's [8, 33, 34], as well as in inorganic magnetic tunneling junctions based on the same two FM electrodes [35-37]. The TMR steep decrease with  $V$  was explained in the latter devices as due to changes in  $P(\text{Co})$  upon sweeping  $V$  [35]; or by the increase of the electron-magnon scattering in the LSMO electrode upon current density increase [38, 39].

### (iii) Magnetoresistance temperature dependence

The temperature dependence of the MR response in OSV made from a variety of organic small molecules and polymers spacers was measured by several groups [8, 17, 19, 23]. It was found that the  $MR_{SV}$  value dramatically decreases with  $T$ . Figure 3(a) shows the  $MR_{SV}$  temperature dependence obtained in three OSV devices based on different OSEC interlayer molecules [23]. These molecules are: Alq<sub>3</sub> with green emission; CVB, discussed above; and N,N'-bis (1-naphthalenyl)-N-N'-bis (phenyl) benzidine [ $\alpha$ -NPD], which is a hole transport layer. It is seen that  $MR_{SV}$  monotonically decreases with  $T$ , and vanishes (within the noise level) at  $T \sim 220\text{K}$  independent of the specific OSEC interlayer.

There are two possible explanations for the  $MR_{SV}$  decrease with  $T$ , namely that the FM electrodes spin polarization degree,  $P$  is temperature dependent; and that the spin-aligned transport through the organic spacer diminishes at high  $T$  due to an increase of spin-lattice relaxation rate for the charge polaron excitations injected into the OSEC layer. The later explanation was somewhat refuted in ref. [23], where it was shown that the spin-lattice relaxation rate in a typical small OSEC molecule (namely  $Alq_3$ ) is in fact temperature independent. However more recent experiments using the technique of low-energy muon spin rotation claim that the spin-lattice relaxation rate in  $Alq_3$  increases with  $T$  [40]. In addition the similarity of the obtained  $MR_{SV}$  response for the different OSEC used above indicates that the FM electrodes response, rather than the particular OSEC interlayer response dominates the  $MR_{SV}$  decrease with  $T$ . The Co magnetic properties do not change much with  $T$ ; however, the LSMO magnetic properties strongly depend on  $T$  (Fig. 3(b) inset) [41, 42], and it was thus concluded that its particular response is the underlying mechanism responsible for the  $MR_{SV}$  temperature dependence in OSV based on this spin-injecting electrode [23].

#### (iv) Spin polarization properties of the LSMO electrode

The MR response of various OSV has been interpreted using a modified Jullière model [43], in which  $MR_{SV}$  ( $= [\Delta R/R]_{\max}$ ) is given by [8]:

$$[\Delta R/R]_{\max} = 2P_1P_2D/(1 + P_1P_2D), \quad (1)$$

where  $P_1$  and  $P_2$  are the spin polarizations of the two FM electrodes, respectively. In Eq. (1)  $D = \exp[-(d-d_0)/\lambda_s]$ , where  $\lambda_s$  is the spin diffusion length in the OSEC,  $d$  is the OSEC thickness and  $d_0$  ( $\sim 60$  nm) is an “ill-defined” OSEC layer thickness [8], where inclusions of the upper, evaporated FM metal may be abundantly found. Eq. (1) is in fact written in the spirit of a more rigorous analysis of MR responses in inorganic semiconductor spin-valves [44, 45], where the

processes of spin injection, spin accumulation, and spin transport through a semiconductor are all explicitly taken into account in the calculation.

As shown in Fig. 3(a) we may calculate the normalized spin polarization value  $P_1(T)$  ( $= P(\text{LSMO})$ ) for the LSMO electrode vs. temperature (Fig. 3(b)) from the  $\text{MR}_{\text{SV}}$  temperature dependence using Eq. (1), assuming that the parameters  $P_2(\text{Co})$  and  $D$  are temperature independent [23]. From our calculation it is seen that  $P(\text{LSMO})$  steeply decreases with  $T$  indicating that the surface spin polarization of the LSMO electrode strongly depends on temperature. For comparison with the FM bulk properties, the LSMO magnetization moment,  $M$  vs. temperature was also measured (Fig. 3(b) inset) [23]. In contrast to  $P(\text{LSMO})$  vs.  $T$  obtained above,  $M(T)$  is less temperature dependent; in particular  $M$  vanishes at a Curie temperature,  $T_c = 325\text{K}$  rather than at  $T \sim 220\text{K}$ , where  $P(\text{LSMO})$  diminishes (Fig. 3(b)). It is thus apparent that the *surface* LSMO spin polarization, rather than the bulk LSMO magnetization is responsible for the steep decrease of  $P(\text{LSMO})$  with  $T$ . In fact the obtained  $P(\text{LSMO})$  temperature response agrees very well with the surface spin polarization of LSMO films as probed by spin-polarized photoemission spectroscopy [41], which measures the polarized charge carrier density at the surface boundary within  $5 \text{ \AA}$  depth.

#### (v) Room temperature LSMO-based OSV operation

There is no real obstacle for obtaining LSMO-based OSV operation at room temperature, provided that the signal/noise (S/N) ratio of the MR loop measurement is improved to observe the weak, anticipated MR signal at  $\sim 300\text{K}$ . To achieve this task the LSMO-based OSV needs be very stable in order to improve the S/N ratio in the MR measurements. We recently found that OSV devices based on  $\text{C}_{60}$  spacer layer indeed possess such stable operation. This is probably caused by a superior interface between the LSMO and  $\text{C}_{60}$  molecular layer that may be formed



due to the ability of the fullerene molecule to diffuse at the deposition temperature, thus filling the LSMO rough surface [46]. Another advantage of the  $C_{60}$  spacer is the weak hyperfine interaction (HFI) of this molecule, which is based only on carbon atom. The carbon nucleus  $^{12}C$  isotope has spin singlet, and thus does not count for the HFI. Although  $^{13}C$  isotope nucleus is spin doublet, nevertheless  $^{13}C$  natural abundance is  $< 2\%$ , and thus the overall HFI of the natural  $C_{60}$  molecule may be  $\sim$  two orders smaller than that of the hydrogen atom. We therefore conjecture that the weak HFI of  $C_{60}$  molecule may increase the spin diffusion length in OSV based on fullerene molecules so that the corresponding MR would be only limited by the LSMO ability of injecting spin-aligned carriers into the OSEC.

Figure 4 shows the MR loop of a LSMO/ $C_{60}$ /Co OSV at room temperature (RT). The excellent S/N ratio achieved in these measurements reveal a  $MR_{SV}$  of  $\sim 0.16\%$  at 200 mV bias; the  $MR_{SV}$  increases to  $\sim 0.3\%$  at low bias voltage, namely  $V < 50$  mV [46]. The obtained  $MR_{SV}$  value is similar to that measured using OSV's with a polymer spacer [19], or superior LSMO surface [17, 21]. This shows that the  $MR_{SV}$  RT value is independent of the OSEC used, or the quality of the LSMO surface; instead it depends on the intrinsic properties of the spin-polarized injection capability of the LSMO substrate at RT, in agreement with section (iv) above. It is also noteworthy that the coercive fields of the LSMO and Co FM electrodes at RT ( $< 80$  Gauss) are both much smaller than the corresponding fields at low temperature [46]; and this makes the OSV devices very attractive for RT applications.

#### **(vi) Improved OSV operation in polymer spacers**

We have synthesized a  $\pi$ -conjugated polymer based on poly-phenylene vinylene derivative, namely DOO-PPV polymer; see Fig. 5 inset), [47]. The advantage of this polymer is that the organic layer can be

spin cast rather than evaporated with small molecules. We showed that this has a profound influence on the magnetoresistance response [47]. We have fabricated OSV based on LSMO/polymer/Co sandwiched configuration with the DOO-PPV polymer as the nonmagnetic spacers [47]. Figure 5(a) shows representative MR hysteresis loops for the polymer OSVs based on DOO-PPV at  $T = 10\text{K}$  and  $V = 20\text{ mV}$ . We found that the SV-related magnetoresistance is positive in such OSV. Most of the MR loops in previous OSV showed negative effect, namely that the resistance is *smaller* when the LSMO and Co magnetization directions were antiparallel to each other. This was originally explained [8] as due to the negative spin polarization,  $P(\text{Co})$  of the Co FM electrode (see Eq. (1)). However it was subsequently measured that  $P(\text{Co})$  is positive [24, 27], raising the question related to the MR sign again. Our positive MR adds to the puzzle, and shows that when the organic interlayer is loosely bound to the FM electrodes, such as fabricated by spin-casting; then the MR response is positive.

#### (vii) OSV based on conventional FM electrodes

In addition to OSV based on LSMO, which has SP injecting capability  $P$  of  $\sim 95\%$ , other OSV devices based on more conventional FM electrodes having smaller  $P$  but less steep temperature dependencies such as Fe, Co and Ni have been also studied [16, 24, 27, 28, 30]. Originally it was reported [16] that OSV based on  $\text{Alq}_3$  interlayer sandwiched between Fe and Co FM electrodes showed  $\text{MR}_{\text{SV}} \sim 3\%$  at low temperature; recently this value was measured to be  $\sim 7\%$  [28]. However more recently the original data [16] was challenged [30]; it was claimed that when *carefully fabricated*, namely deposition in a chamber of high vacuum and without breaking the vacuum in between the OSEC and electrodes deposition, then the OSV does not show spin-valve MR response [30]. This claim has casted some doubts on the obtained MR response in OSV in general, since the response might have been due to artifacts such as FM inclusions in the OSEC film as claimed in ref. [20]; although numerous laboratories around the world have repeated the original OSV response data [8]. These doubts, however were refuted very recently when the spin

diffusion length in an amorphous OSEC film of rubrene ( $C_{42}H_{28}$ ) of SP electrons injected from conventional FM electrodes was directly obtained by spin polarized tunneling into an Al superconductor film at ultralow temperature [27]. A spin diffusion length of  $\sim 13$  nm was measured at low temperature with relatively small decrease up to room temperature; and the authors predicted a spin diffusion length of few nm in rubrene single crystal [27]. Moreover a  $MR_{SV}$  of  $\sim 15\%$  was measured for an OSV composed of Co/ $Al_2O_3$ /rubrene/Fe magnetic tunneling junction, in which a tunnel barrier layer was introduced between the Co and OSEC interlayer [27]; this is in direct contradiction with the claims in ref. [30], which argued a null MR response for OSV made of conventional FM electrodes, even when a tunnel barrier was introduced between one of the FM electrode and OSEC layer. In addition very recently Liu *et. al* reported measurements on Fe/ $Alq_3$ /Co OSV [28]. It was found that a correlation exists between the MR and the FM/ $Alq_3$  interface microstructure. It was concluded that is possible to realize room temperature spin injection into the OSEC layer from electrodes made of transition metals by careful interface modification.

### 3. A Theoretical insight

A recent excellent theoretical review dealt with the MR response of OSV under different growing conditions [3]. In that contribution the SP injection current was calculated and compared to the charge current in diverse organic diodes based on: (1) conventional FM electrodes without a tunnel barrier; (2) conventional FM with a tunnel barrier (insulating buffer layer) between the FM electrode and OSEC interlayer; and (3) electrode composed of half metallic FM materials with low conductivity, such as LSMO. It was shown [3] that spin injection is indeed difficult to achieve for case (1) since the “conductivity mismatch” [12-14] acts for OSEC similarly as for inorganic semiconductors. This may explain the reason that MR was not achieved in OSV devices based on two conventional FM electrodes without a tunnel barrier in between the FM electrode and OSEC layer [30]. However according to the model used, the SP



current *dramatically increases* in case (2) when a tunnel barrier is introduced and thus spin-dependent tunneling is the limiting process for spin-polarized carrier injection. This explains the earlier result [16], where a tunnel barrier was inadvertently introduced between the OSEC and the capped FM layer (Co), due to the fabrication process; in that case the vacuum in the evaporation chamber was broken before evaporating the upper FM electrode. It also explains the more recent finding [28] where a dead magnetic region was seen to occur near the Fe electrode, which resulted in an excellent MR value for Fe/Alq<sub>3</sub>/Co spin valve. Moreover it was also shown in the theoretical work [3] that SP current is *substantial* in case (3) for half-metallic FM, because its conductivity is low (thus reducing the conductivity mismatch with the OSEC interlayer), and its *P* value is close to 100%. This explains the high MR response in OSV based on LSMO as a SP injecting electrode, such as in ref. [8] without the need of using tunnel barriers.

#### 4. Conclusions and Future Outlook

In this contribution we reviewed some of the latest achievements in organic spin valves research at the University of Utah. The Organic Spintronics field is in its infancy; much more work has to be accomplished before the field would mature. At the present time controversies regarding the exact operation of OSV still exist; especially the MR signs in these devices. Recently SP carrier injection into an OSEC has been directly observed using low-energy muon spin rotation [40]; so the doubts raised at the beginning of the Organic Spintronics field may be well defused. In general spin injection achieved in OSV is of the same magnitude as in spin-valves fabricated using inorganic semiconductor spacers. In particular both organic and inorganic semiconductor interlayer suffer from the same conductivity mismatch problem, and show only little MR at room temperature.

OSEC do not possess the polarized emission properties of inorganic semiconductors such as GaAs, which can be used to directly detect SP current in spin-valve devices [49]. The reason for that is that the emission in OSEC results from tightly bound singlet excitons [50], rather than pairs of electrons and holes as is the typical case in inorganic semiconductors. Also the method of spin induced magnetic Kerr effect, which has been successfully used to image SP carrier injection into inorganic semiconductors [51] is not useful for OSV, because of the small current involved, and the small spin orbit coupling in the OSEC layer. Direct imaging of SP current injection into OSEC is highly needed because MR alone may be prone to artifacts [52]. Therefore other detection methods are needed that are capable of more directly measure depth resolved information on the SP charge carriers within the buried layers of organic spin devices. Such a method was recently reported [40, 53] using low energy muon spin rotation. Other methods such as two-photon photoemission have been also recently advanced to probing spin injection into OSEC [54]. The field of organic spintronics has very much benefited from such direct measurements of spin injection [53].

Room temperature MR of less than 1% has been achieved with OSV based on LSMO; this is too low for generating industrial interest. For this field to take off, FM spin-injector other than LSMO need be discovered, of which high SP injection capabilities would survive at room temperature. We predict that it should be possible to reach sizable room temperature  $MR_{SV}$  values in OSV based on FM electrodes with large  $P$ , but with a milder dependence on temperature than the LSMO. Such a FM electrode, for example might be the half metallic  $CrO_2$  with  $T_c \cong 395K$  [55], although no spin-valve devices based on it have been successful so far; or the double-perovskite oxides with  $T_c > 400K$  [56]; or the recently discovered  $EuO$  [57]. It is also noteworthy that OSV with room temperature MR of few % has been recently measured in  $Fe/Alq_3/Co$  OSV [28]. Another possibility would be to use *organic* FM as spin injecting electrodes [58]. Since the conductivity of these FM materials matches that of OSEC, the



conductivity mismatch problem would be naturally resolved. We also note that sizable SP carrier injection was recently achieved in graphene [59], which is a single layer graphite, but still could be considered as an OSEC material.

### **Acknowledgements**

This work was supported in part by US Department of Energy Grant No. 04-ER 46109 at the University of Utah. ZVV acknowledges the support of The Lady Davis Fellowship Trust while on sabbatical at the Technion, Israel.

### **References**



- [1] S. A. Wolf, D. D. Awschalom, R. A. Buhrman, J. M. Daughton, S. von Molnar, M. L. Roukes, A. Y. Chtchelkanova, and D. M. Treger, *Science* 294 (2001) 1488.
- [2] I. Zutic, J. Fabian, and S. Das Sarma, *Rev. Mod. Phys.* 76 (2004) 323.
- [3] M. Yunus, P. P. Ruden, and D. L. Smith. *Jour. of Appl. Phys.* 103 (2008) 103714.
- [4] V. Dediu, M. Murgia, F. C. Maticotta, C. Taliani, and S. Barbanera, *Solid State Commun.* 122 (2002) 181.
- [5] S. Sanvito and A. R. Rocha, *Jour. of Computational and Theoretical Nanoscience* 3 (2006) 624.
- [6] W. J. M. Naber, S. Faez, and W. G. van der Wiel, *J. Phys : Appl. Phys* 40 (2007) R205.
- [7] B. T. Jonker, *Proc. IEEE* 91(2003) 727.
- [8] Z. H. Xiong, D. Wu, Z. V. Vardeny, and J. Shi, *Nature (London)* 427 (2004) 821.
- [9] D. D. Awschalom and M. E. Flateé, *Nature Phys.* 3 (2007) 153.
- [10] X. Lou, C. Adelman, S. A. Crooker, E. S. Garlid, J. Zhang, S. M. Reddy, S. D. Flexner, C. J. Palmström, and P. A. Crowell, *Nature Phys.* 3 (2007) 197.
- [11] S. Sanvito, *Nature Mater.* 6 (2007) 803.
- [12] G. Schmidt, D. Ferrand, L. W. Molenkamp, A. T. Filip, and B. J. van Wees, *Phys. Rev. B* 62 (2000) R4790.
- [13] E. I. Rashba, *Phys. Rev. B* 62 (2000) R16267.
- [14] D. L. Smith and R. N. Silver, *Phys. Rev. B* 64 (2001) 045323.
- [15] J. D. Albrecht and D. L. Smith, *Phys. Rev. B* 66 (2002) 113303.
- [16] F. J. Wang, Z. H. Xiong, D. Wu, J. Shi, and Z. V. Vardeny, *Synth. Met.* 155 (2005) 172.



- [17] V. Dediu, L. E. Hueso, I. Bergenti, A. Riminucci, F. Borgatti, P. Graziosi, C. Newby, F. Casoli, M. P. De Jong, C. Taliani, and Y. Zhan, *Phys. Rev. B* 78 (2008) 115203.
- [18] T. X. Wang, H. X. Wei, Z. M. Zeng, X. F. Han, Z. M. Hong, and G. Q. Shi, *Appl. Phys. Lett.* 88 (2006) 242505.
- [19] S. Majumdar, H. S. Majumdar, P. Laukkanen, I. J. Väyrynen, R. Laiho, and R. Österbacka, *Appl. Phys. Lett.* 89 (2006) 122114.
- [20] W. Xu, G. J. Szulczewski, P. LeClair, I. Navarrete, R. Schad, G. Miao, H. Guo, and A. Gupta, *Appl. Phys. Lett.* 90 (2007) 072506.
- [21] L. E. Hueso, I. Bergenti, A. Riminucci, Y. Zhan, and V. Dediu, *Adv. Mater.* 19 (2007) 2639.
- [22] S. Pramanik, C. -G. Stefanita, S. Padibandla, S. Bandyopadhyay, K. Garre, N. Harth, and M. Cahay, *Nature Nanotech.* 2 (2007) 216.
- [23] F. J. Wang, C. G. Yang, Z. Vally Vardeny, and X. G. Li, *Phys. Rev. B.* 75 (2007) 245324.
- [24] T. S. Santos, J. S. Lee, P. Migdal, I. C. Lekshmi, and J. S. Moodera, *Phys. Rev. Lett.* 98 (2007) 016601.
- [25] N. A. Morley, A. Rao, D. Dhandapani, M. R. J. Gibbs, M. Grell, and T. Richardson, *J. Appl. Phys.* 103 (2008) 07F306.
- [26] F. J. Wang, Z. Vally Vardeny, *J. Mater. Chem.*, 19 (2009) 1685
- [27] J. H. Shim, K. V. Raman, Y. J. Park, T. S. Santos, G. X. Miao, B. Satpati, and J. S. Moodera, *Phys. Rev. Lett.* 100 (2008) 226603.
- [28] Y. Liu, S. M. Watson, T. Lee, J. M. Gorham, H. E. Katz, J. A. Borchers, H. D. Fairbrother, and D. H. Reich, *Phys. Rev. B* 79 (2009) 075312.
- [29] M. Bowen, M. Bibes, A. Barthélémy, J. P. Contour, A. Anane, Y. Lemaitre, and A. Fert, *Appl. Phys. Lett.* 82 (2003) 233.





- [30] J. S. Jiang, J. E. Pearson, and S. D. Bader, *Phys. Rev. B* 77 (2008) 035303.
- [31] D. Wu, Z. H. Xiong, X. G. Li, Z. V. Vardeny, and J. Shi, *Phys. Rev. Lett.* 95 (2005) 016802.
- [32] Y. C. Zhang, M. P. deJong, F. H. Li, V. Dediu, M. Fahlman, and W. R. Salaneck, *Phys. Rev. B* 78 (2008) 045208.
- [33] A. Riminucci, I. Bergenti, L. E. Hueso, M. Muriga, C. Taliani, Y. Zhan, F. Casoli, M. P. de Jong, and V. Dediu, *cond-mat/0701603* (2007).
- [34] L. E. Hueso, J. M. Pruneda, V. Ferrari, G. Burnell, J. P. Valdés-Herrera, B. D. Simons, P. B. Littlewood, E. Artacho, A. Fert, and N. D. Mathur, *Nature* 445 (2007) 410.
- [35] J. M. De Teresa, A. Barthélémy, A. Fert, J. P. Contour, F. Montaigne, and P. Seneor, *Science* 286 (1999) 507.
- [36] J. S. Moodera and G. Mathon, *Jour. Magnetism and Magnetic Materials* 200 (1999) 248.
- [37] J. Hayakawa, K. Ito, S. Kokado, M. Ichimura, A. Sakuma, M. Sugiyama, H. Asano, and M. Matsui, *J. Appl. Phys.* 91 (2002) 8792.
- [38] S. Zhang, P. M. Levy, A. C. Marley, and S. S. P. Parkin, *Phys. Rev. Lett.* 79 (1997) 3744.
- [39] A. M. Bratkovsky, *Phys. Rev. B* 56 (1997) 2344.
- [40] A. J. Drew, J. Hoppler, L. Schulz, F. L. Pratt, P. Desai, P. Shakya, T. Kreouzis, W. P. Gillin, A. Suter, N. A. Morley, V. K. Malik, A. Dubroka, K. W. Kim, H. Bouyanfif, F. Bourqui, C. Bernhard, R. Scheuermann, G. J. Nieuwenhuys, T. Prokscha & E. Morenzoni. *Nat. Mater.* 8 (2009) 109.
- [41] J. -H. Park, E. Vescovo, H. -J. Kim, C. Kwon, R. Ramesh, and T. Venkatesan, *Phys. Rev. Lett.* 81 (1998) 1953.

- [42] V. Garcia, M. Bibes, A. Barthélémy, M. Bowen, E. Jacquet, J. -P. Contour, and A. Fret, Phys. Rev. B 69 (2004) 052403.
- [43] M. Julliere, Phys. Rev. A 54 (1975) 225.
- [44] A. Fert and H. Jaffrès, Phys. Rev. B 64 (2001) 184420.
- [45] A. Fert, J. -M. George, H. Jaffrès, and R. Mattana, cond-mat/0612495 (2006).
- [46] F. J. Wang, PhD thesis, University of Utah, January (2009) (unpublished).
- [47] T. D. Nguyen, G. Hukic-Markosian, F. J. Wang, L. Wojcik, X.-G. Li, E. Ehrenfreund and Z. V. Vardeny, submitted.
- [48] P. A. Bobbert, W. Wagemans, F. W. A. van Oost, B. Koopmans, and M. Wohlgenannt, Phys. Rev. Lett. 102 (2009) 156604.
- [49] (a) R. Flederling, M. Kelm, G. Rauscher, W. Ossau, G. Schmidt, A. Waag, and L. W. Molenkamp, Nature 402 (1999) 787. (b) Y. Ohno, D. K. Young, B. Beschoten, F. Matsukura, H. Ohno, and D. D. Awschalom, *ibid*, 790.
- [50] S. Singh, T. Drori, and Z. V. Vardeny, Phys. Rev. B 77 (2008) 195304.
- [51] S. A. Crooker, M. Furis, X. Lou, C. Adelmann, D. L. Smith, C. J. Palmstrøm, P. A. Crowell, Science 309 (2005) 2191.
- [52] J. M. Coey, Jour. Appl. Phys. 85 (1999) 5576.
- [53] Z. V. Vardeny, Nat. Mater. 8 (2009) 91.
- [54] M. Cinchetti, K. Heimer, J-P Wüstenberg, O. Andreyev, M. Bauer, S. Lach, C. Ziegler, Y. Gao, and M. Aeschlimann, Nature Mater. 8 (2009) 115.
- [55] R. S. Keizer, S. T. B. Goennenwein, T. M. Klapwijk, G. Miao, G. Xiao, and A. Gupta, Nature 439 (2006) 825; and references therein.



[56] D. Serrate, J. M. De Teresa, and M. R. Ibarra, *J. Phys.: Condens. Matter* 19 (2007) 023201.

[57] J. F. Gregg, *Nature Mater.* 6 (2007) 798.

[58] E. Carlegrim, A. Canciurzewska, P. Nordblad, and M. Fahlman, *Appl. Phys. Lett.* 92 (2008) 163308.

[59] N. Tombros, C. Jozsa, M. Popinciu, H. T. Jonkman, and B. J. van Wees, *Nature* 448 (2007) 571.

## Figure Captions

**Fig. 1** (a) The  $I$ - $V$  characteristic response of LSMO/CVB(102nm)/Co/Al diode at three temperatures: 14K (dark circles), 140K (dark stars), and 200K (black squares). The upper inset shows schematically the organic spin valve device and magnetoresistance measurement configuration, where  $I$  and  $V$  are the injected current and biasing voltage across the device, respectively, and  $H$  is the external in-plane magnetic field. The lower inset shows the chemical structure of the CVB molecule. (b) The magnetoresistance response of the spin-valve device shown in (a) for an applied biasing voltage of 10 mV at 14K; the empty squares (filled circles) are for  $H$  swept in the forward (backward) direction. The arrows show the relative magnetization directions of the FM electrodes at various  $H$ , in relation with the FM coercive fields. Reproduced in part from ref. 23; copyright 2007 American Physical Society. Used with permission.

**Fig. 2** The spin-valve related MR value of the diode shown in Fig. 1 vs. the applied biasing voltage,  $V$  at 14K (filled circles) and 140K (empty circles); the 140K data were multiplied by a factor of 2.8 for normalization purpose. Reproduced in part from ref. 23; copyright 2007 American Physical Society. Used with permission.

**Fig. 3** (a) The MR value of three different LSMO/OSEC/Co spin valve devices vs. temperature,  $T$  normalized at  $T = 14$ K. The OSEC interlayers in these devices are: Alq<sub>3</sub> (squares); CVB (circles); and NPD (stars); their chemical formulae are given in the text. (b) The calculated LSMO spin polarization,  $P(\text{LSMO})$  using the modified Jullière model [8] (Eq. (1) in the text) and the data in (a); the symbols and colors are the same as in (a) above. The line through the data

points is the calculated polarized charge carrier density (PCCD) of the LSMO electrode normalized at  $T = 0$  using the model given in ref. 37, with  $T_c = 325\text{K}$ . The inset shows the magnetization,  $M$  (empty circles) of the LSMO film used as the bottom FM electrode for the OSV shown in (a); the Curie temperature,  $T_c = 325\text{K}$  is assigned. Reproduced in part from ref. 23; copyright 2007 American Physical Society. Used with permission.

**Fig. 4** The MR response of an OSV based on 40 nm thick  $\text{C}_{60}$  spacer layer in between LSMO and Co FM electrodes at room temperature and bias voltage  $V = 200\text{ mV}$ .

**Fig. 5** The MR response of an OSV device based on 40 nm thick DOO-PPV spacer layer in between LSMO and Co FM electrodes measured at temperature of 10 K and bias voltage  $V = 20\text{ mV}$ ; the polymer backbone structure is shown in the inset.

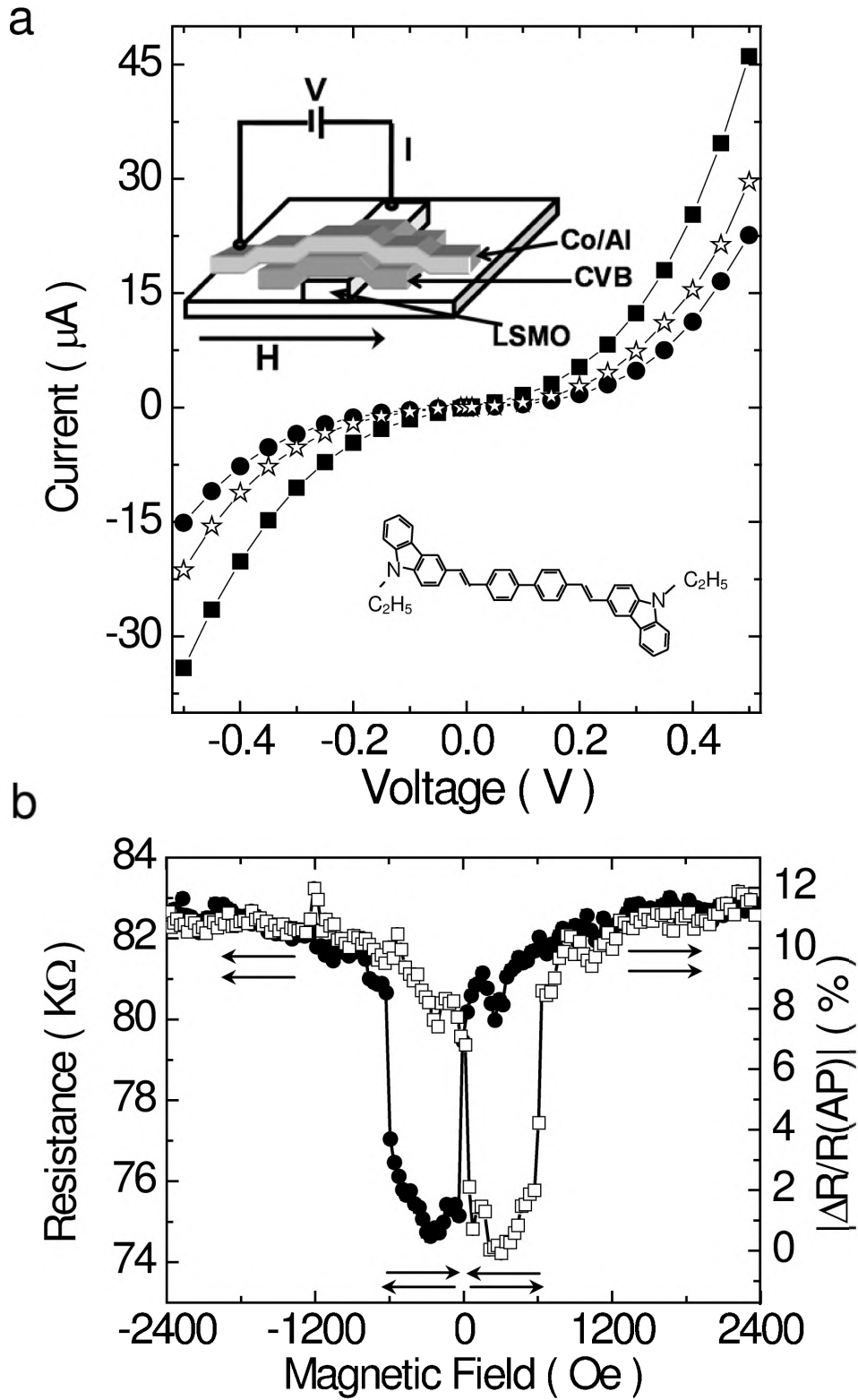


Figure 1

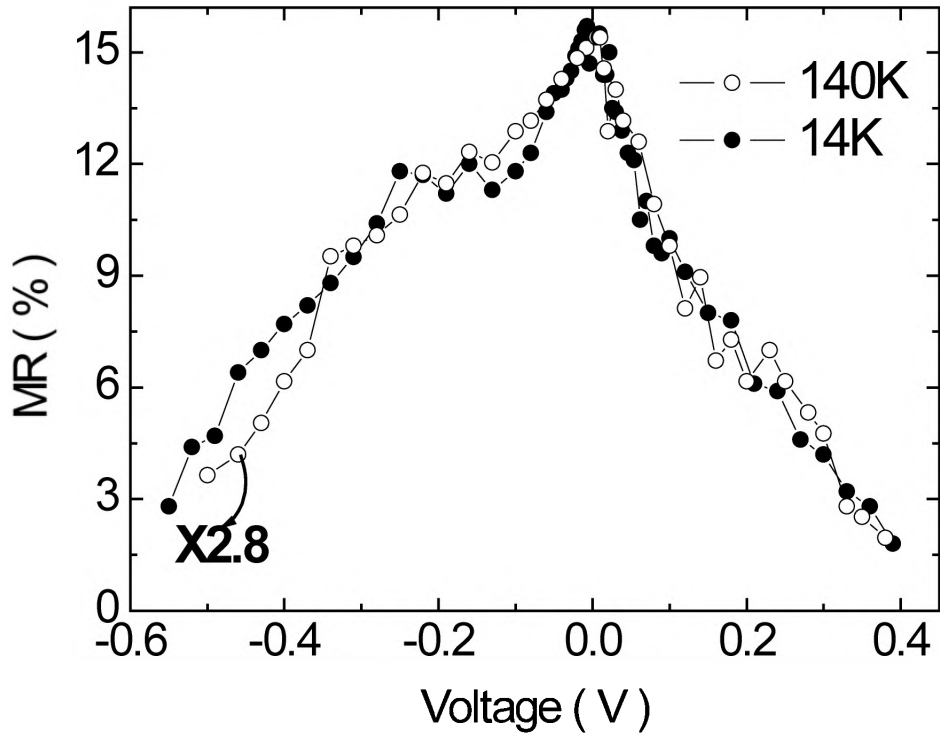


Figure 2

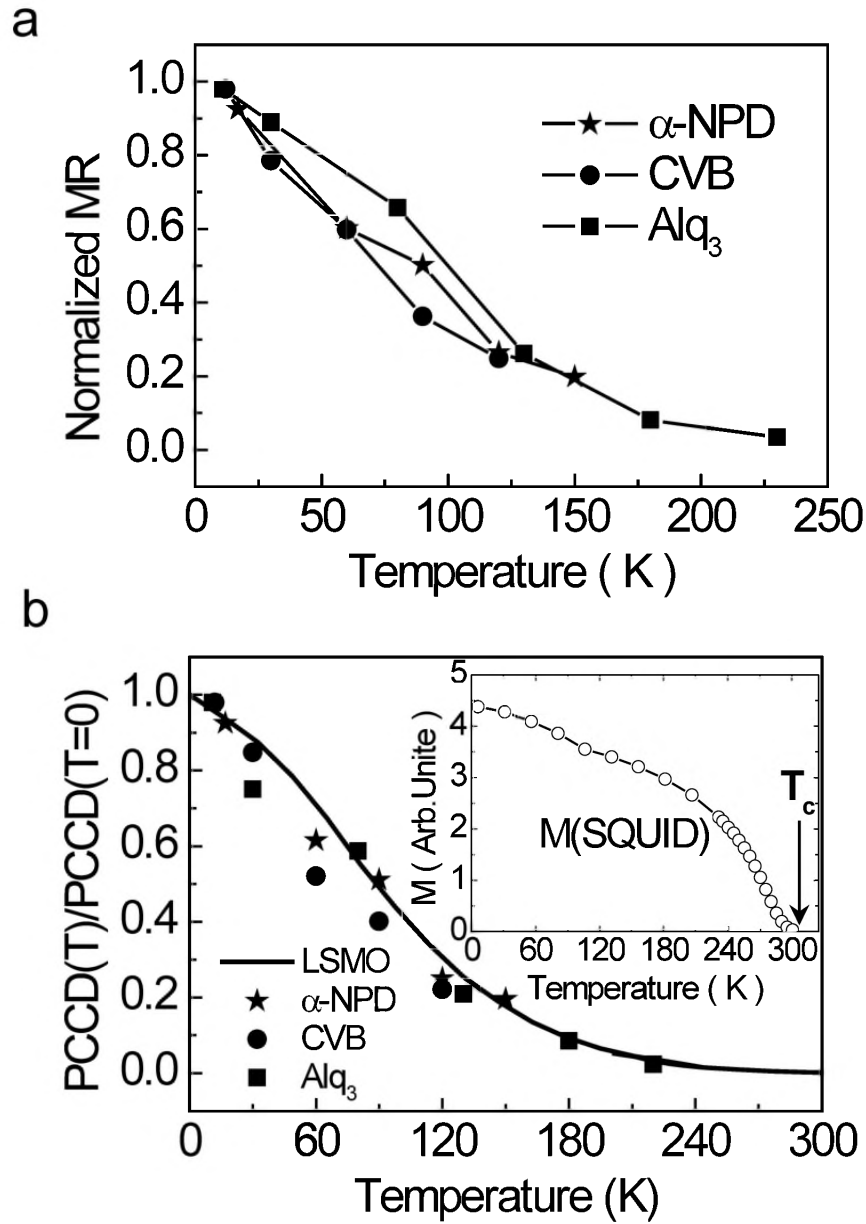


Figure 3



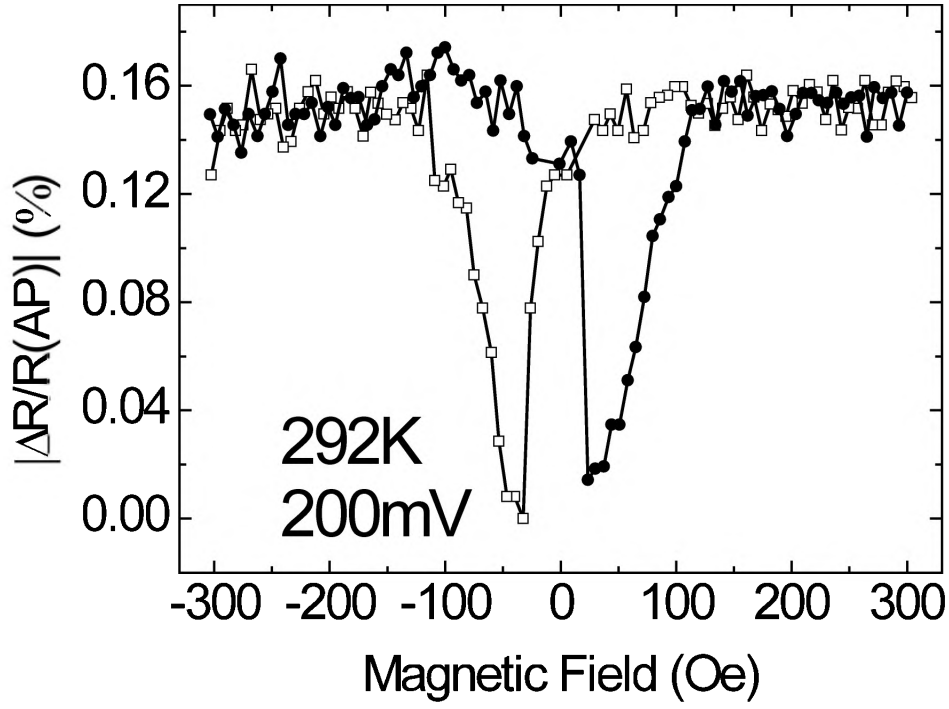


Figure 4

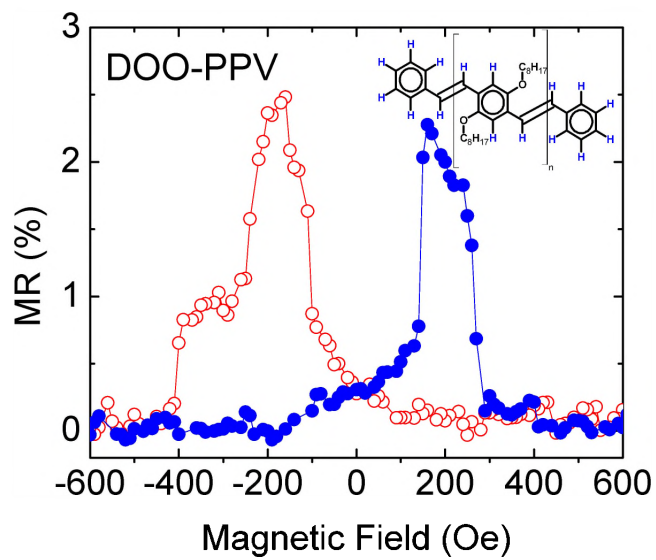


Figure 5

**Fig. 5** The MR response of an OSV device based on 40 nm thick DOO-PPV spacer layer in between LSMO and Co FM electrodes measured at temperature of 10 K and bias voltage  $V = 20$  mV; the polymer backbone structure is shown in the inset.